SAND2019-1818R

U.S. DEPARTMENT OF ENERGY

Sandia National Laboratories

Solid Rocket Motor Design using a Low-Dimensional Fluid Model

M.A. Aguilo, S.W. Bova and D.R. Noble

Sandia National Laboratories
Albuquerque, NM

February 12, 2019

1 Introduction

This document is a summary of the mathematical models that are used in the DARPA TRADES project for the solid rocket motor design challenge. It is hoped that this brief description of these models will be of use to those that are working on the project.

2 Overview

Consider the schematic of a cross section of a model of a solid rocket motor as shown in Figure 1. The model consists of two volumes: a combustion chamber which consists of a solid propellant and a gas, and an attached nozzle. Let the walls of the motor case be denoted by Γ_w. The volume of propellant contained within is denoted by $\Omega_p(t)$. There is a cavity, $\Omega_f(t)$, within the motor, which contains a gas. The gas and the solid are separated by a surface which we denote $\Gamma_p(t)$. Let Γ_e and Γ_d denote artificial boundaries in the exit and inlet planes of the nozzle, respectively. Γ_w, Γ_e and Γ_d do not change with time.

We assume that the system is at some known, quiescent state, so that at time $t = 0$, $\Omega_p(t)$, $\Omega_f(t)$, and $\Gamma_p(t)$ are well-defined. At a certain later time, the propellant is ignited, and the mass of the combustion products enter $\Omega_f(t)$ as the surface $\Gamma_p(t)$ recedes. This increase in the mass of Ω_f creates a pressure increase and causes the motor to generate thrust. Given Γ_w, the problem is to design the initial shape of Ω_p, or equivalently, Γ_p, to produce the desired thrust as a function of time.

2.1 Conservation of mass

The principle of conservation of mass within a time-dependent control volume $\Omega(t)$ with boundary $\partial\Omega(t)$ may be written as a mathematical equation in integral

Sandia National Laboratories is a multimission laboratory managed and operated by National Technology & Engineering Solutions of Sandia, LLC, a wholly owned subsidiary of Honeywell International Inc., for the U.S. Department of Energy's National Nuclear Security Administration under contract DE-NA0003525. SAND2019-XXXX

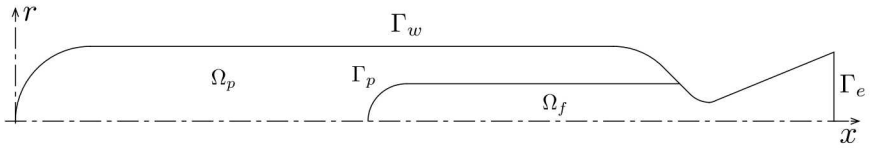

Figure 1: A representation of a cross section of a solid rocket motor. The centerline is given by the x axis. The propellant volume, Ω_p, is not necessarily axisymmetric.

form:

$$\partial_t \int_{\Omega(t)} \rho \, dV = - \int_{\partial\Omega(t)} \dot{m} \, dS, \tag{1}$$

where ρ is the density of gas in $\Omega(t)$, and $\dot{m}$ is the mass flux through the boundary.

Let a combustion chamber consist of a cavity with an initial volume V_0, bounded by a closed surface

$$\partial\Omega(t) = \Gamma_p(t) \cup \Gamma_d \tag{2}$$

where $\Gamma_p(t)$ is the time-varying surface of the solid propellant, and Γ_d denotes an arbitrary dividing surface between the chamber and the nozzle that does not change with time. If we are only interested in the average properties within the cavity, we can introduce the average density

$$V = \int_{\Omega(t)} dV \tag{3}$$

$$\bar{\rho} = \frac{\int_{\Omega(t)} \rho \, dV}{V} \tag{4}$$

$$\tag{5}$$

Now the mass conservation equation (1) may be written as

$$d_t(\bar{\rho} V) = - \int_{\Gamma_p} \dot{m} \, dS - \int_{\Gamma_d} \dot{m} \, dS, \tag{6}$$

where it should be understood that $\Gamma_p = \Gamma_p(t)$, and that $d_t()$. indicates that a quantity is differentiated with respect to time, its only variable.

2.2 A quasi-steady gas model

For the class of propellants considered in this work, the burn rate is on the order of 1 centimeter per second. When the gas leaves the exit plane of the nozzle, it has been accellerated to a few thousand meters per second. Therefore the time

scales associated with the surface recession are much longer than the response time of the gas in the nozzle, and a quasi-steady assumption might be useful under certain circumstances. In this case,

$$d_t \bar{\rho} V = 0$$

and the lack of a capacitance term in the equations allows the mass flow across the propellant surface to be equated to the mass flow across Γ_d, which is chosen to be the cross-sectional surface at the nozzle throat. The resulting model is described by Kibbey [1], and we can write it as follows.

$$\int_{\Gamma_p(t)} \dot{m}\, dS = -\int_{\Gamma_d} \dot{m}\, dS = a_* p_t / c_* \tag{7}$$

where a_* is the area of the throat, c_* is a known constant characteristic velocity of the nozzle, and p_t is the unknown pressure inside the chamber. Equation (7) follows from the fact that there is an analytic solution for the quasi one-dimensional equations for the isentropic flow of an ideal gas in a nozzle[2]. Under these conditions, p_t is a value that does not vary in space, but may vary in time.

The mass flux into the combustion chamber is modeled as

$$\dot{m} = \rho_p \dot{r}_r(x, y, z) \left(\frac{p_t}{p_r} \right)^{\alpha} \tag{8}$$

In (8), ρ_p is the given density of the propellant, $\dot{r}_r(x, y, z)$ is a known reference burn rate distribution, $\alpha = 0.38$ and p_r is a known reference pressure. For propellants of interest in this study, $2.5\,\text{mm/s} < \dot{r}_r < 15.25\,\text{mm/s}$, and $P_r = 3.447 \times 10^6$ Pa. If we substitute (8) into (7) we get a nonlinear equation for the pressure in the combustion chamber. We can solve this equation using Newton's method. Define the residual

$$f = \int_{\Gamma_p(t)} \rho_p \dot{r}_r(x, y, z) \left(\frac{p_t}{p_r} \right)^{\alpha} dS - a_* p_t / c_* = 0 \tag{9}$$

Application of Newton's method to (9) leads to

$$\frac{\partial f}{\partial p_t} \Delta p_t = -f \tag{10}$$

$$\frac{\partial f}{\partial p_t} = \int_{\Gamma_p(t)} \rho_p \dot{r}_r(x, y, z) \frac{\alpha p_t^{\alpha - 1}}{p_r^{\alpha}} dS - a_* / c_* \tag{11}$$

After obtaining the chamber pressure p_t, the thrust, $\mathcal{T}$, can be computed according to

$$\mathcal{T} = I_s g a_* p_t / c_* \tag{12}$$

where g is the constant accelleration of gravity and I_s is the known, constant specific impulse of the rocket in question.

When evaluating (9), the main difficulty is associated with computing the surface integral over $\Gamma_p(t)$. In general, $\Gamma_p(t)$ is a complex surface that varies

in all three space dimensions, as well as time. For the general case, a surface evolution model such as a level set method is needed. We discuss such an approach in Section 3, but for now it is instructive to consider a much simpler case.

2.3 Cylindrical combustion chambers

If we restrict our attention to the case where Γ_p is a cylindrical surface of initial radius r_0 and length L, then the evaluation of (9) is greatly simplified. We also neglect any burning of the circular end surface so that L is assumed to be constant. If we assume that the propellant is of a single type so that $r_r(x, y, z) = r_p$ is a constant value, then we may write

$$\int_{\Gamma_p(t)} \rho_p \dot{r}_r(x, y, z) \left(\frac{p_t}{p_r}\right)^{\alpha} dS \simeq 2\pi L r(t) \rho_p \dot{r}_p \left(\frac{p_t}{p_r}\right)^{\alpha} \tag{13}$$

Then we may write (9) and (11) as

$$f = 2\pi L r(t) \rho_p \dot{r}_p \left(\frac{p_t}{p_r}\right)^{\alpha} - a_* p_t / c_* = 0 \tag{14}$$

$$\frac{\partial f}{\partial p_t} = 2\pi L r(t) \rho_p \dot{r}_p \frac{\alpha p_t^{\alpha-1}}{p_r^{\alpha}} - a_* / c_* \tag{15}$$

where the radius is given by

$$r(t) = r_0 + \dot{r}_p t \tag{16}$$

2.4 Optimization

3 Surface model

Multiple types of level set functions have been used to describe implicit interfaces. One common approach is to use a signed distance function. The magnitude of the function indicates the distance from the nearest interface, and the sign indicates which side of the interface. Another approach, used in conserative level set methods, is to use the hyperbolic tangent of the signed distance function. This second approach is taken here, to take advantage of the relationship with density methods for optimization. The level set function, ψ, is given in terms of the signed distance function, ϕ according to

$$\psi = \frac{1}{2}\left(1 + tanh\left(\frac{\phi}{2\epsilon}\right)\right). \tag{17}$$

This function smoothly transitions from 0 to 1 over a region of thickness of $O(\epsilon)$. The level set value of $\psi = \frac{1}{2}$ indicates the location of the interface. The level set equation evolves using a standard advection equation,

$$\frac{\partial \psi}{\partial t} + \mathbf{u} \cdot \nabla \psi = 0 \tag{18}$$

where the velocity,

$$\mathbf{u} = e\mathbf{n} \tag{19}$$

is in terms of the scalar speed, e, and the level set normal direction,

$$\mathbf{n} = \frac{\nabla\psi}{|\nabla\psi|}. \tag{20}$$

Plugging these into the advection equation gives,

$$\frac{\partial\psi}{\partial t} + e\,|\nabla\psi| = 0. \tag{21}$$

As in all level set methods, this advection equation moves the interface with the given speed but does not maintain the desired properties of the function. In the case of signed distance functions, the signed distance property must be restored through reinitialization. Here, the hyperbolic tangent property must be restored. Specifically we seek a reinitialization equation for restoring a propterty of the gradient of a function that satisfies Eq. 17:

$$\frac{d\psi}{d\phi} = \frac{\psi\,(1-\psi)}{\epsilon}. \tag{22}$$

If ϕ is a signed distance function, then it satifies the property, $|\nabla\phi| = 1$. This means that ψ should satisfy the property,

$$|\nabla\psi| = \frac{\psi\,(1-\psi)}{\epsilon}. \tag{23}$$

Multiple papers have been written on the topic of reinitializing signed distance function and hyperbolic tangent-based level set functions. Because the hyperbolic tangent function was proposed in the context of conservative level set methods, conservative forms have been proposed for the reinitialization equation. Conservative forms are written in flux form that allows for a conservative formulation that guarantees that the integral of the level set field over the domain is the same before and after the reinitialization. Care must be taken, however, when implementing the fluxes to simultaneously maintain monotonicity and conservation. In the current application we are considering surface recession. While we seek to conserve mass in a convergent way, we are not seeking to conserve volume. Consequently, we propose a simpler, non-conservative form for the reinitialization equation:

$$\frac{\partial\psi}{\partial\tau} + \left(\psi - \frac{1}{2}\right)\left(|\nabla\psi| - \frac{\psi\,(1-\psi)}{\epsilon}\right) = 0. \tag{24}$$

Here τ is a pseudo-time variable. Equation 24 is solved to steady state to restore the hyperbolic tangent gradient property to the level set function. In the end each time step involves the explicit evolution of level set field followed by marching the explicit reinitialization equation to steady state. With backward

Euler time integration, mass lumping this involves the an explicit equation for the predicted level set field, $\tilde{\psi}^{n+1}$,

$$\tilde{\psi}_i^{n+1} = \psi_i^n - \Delta t \frac{\int |\nabla \phi| \, e dV}{\int dV} \tag{25}$$

followed by a correction, or reinitialization, in which the iteration is initialized with $\psi_i^{k=0} = \tilde{\psi}_i^{n+1}$, and then the explicit equation

$$\psi_i^{k+1} = \psi_i^k - \Delta\tau \left(\psi_i^k - \frac{1}{2}\right) \left(\frac{\int |\nabla \psi| \, dV}{\int dV} - \frac{\psi_i^k \left(1 - \psi_i^k\right)}{\epsilon} \right) \tag{26}$$

is used until steady-state is reached. This iteration produces the update level set field, $\psi_i^{n+1} = \psi_i^{k=\infty}$. In practice this iteration can be terminated when the updates are small compared to the change in the level set field over the time step.

The hyperbolic tangent form of the level set function is useful for evaluating volume and surface integrals of the evolving domains. The mass of the material on the "positive" side of the interface can be obtained using

$$m_p(t) = \int_{\Omega_p(t)} \rho dV = \int \rho \psi dV \tag{27}$$

The integral of a quantity, γ over the interface can be obtained using,

$$\int_{\Gamma_p(t)} \gamma dS = \int \gamma \, |\nabla \psi| \, dV \tag{28}$$

4 An unsteady gas model

4.1 Governing equations

The fluid region Ω_f has been isolated from Figure 1 and is shown in Figure 2. At any given location x, Ω_f has cross-sectional area $a(x)$. Furthermore, $a(x)$ has perimeter $\ell(x)$. We consider an ideal gas, and invoke the quasi-one-dimensional flow approximation, which states that the flow properties are uniform at any given cross section, e.g. see [2]. If the flow inside the nozzle is further assumed to be inviscid, then we may write the quasi-one-dimensional Euler equations as

$$\begin{aligned}
\partial_t(\rho a) + \partial_x(\rho u a) &= \dot{m}\ell(x) && (29)\\
\partial_t(\rho u a) + \partial_x\left[\left(\rho u^2 + p\right) a\right] &= p\partial_x a && (30)\\
\partial_t(\rho e_t a) + \partial_x\left[u\left(\rho e_t + p\right) a\right] &= -p\partial_t a + \dot{m}\ell(x) e_p && (31)
\end{aligned}$$

where u is the velocity in the x direction, ρ is the density of the gas, p is the pressure of the gas, and e_t is the total specific energy. The mass flux through Γ_p is given by

$$\dot{m} = \rho_p \dot{r}_r \left(\frac{p}{p_r}\right)^\alpha$$

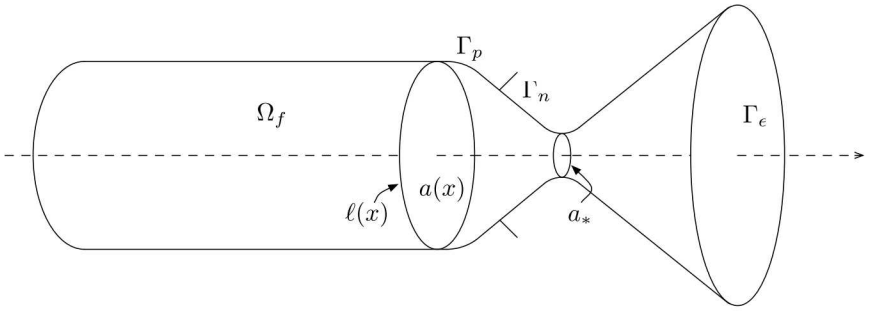

Figure 2: The gas region is denoted Ω_f and is bounded by the propellant surface, Γ_p, the nozzle wall, Γ_n, and the nozzle exit plane, Γ_e. Γ_p is a function of time, but Γ_n is not.

and the time rate of change of the cross-sectional area is computed according to

$$\partial_t a = \ell(x)\dot{r}_r \left(\frac{p}{p_r}\right)^{\alpha} \tag{32}$$

We have chosen to neglect any contribution of momentum carried across Γ_p by the propellant. The first term on the right hand side of (31) is the work done on the gas as the cross-sectional area expands. The second term represents the energy of the propellant gasses that cross Γ_p.

For an ideal gas, the following relations hold:

$$p = \rho R T \tag{33}$$
$$e = c_v T \tag{34}$$

where e is the specific internal energy and T is the temperature. For a given gas, the constant, R and specific heat at constant volume, c_v, are known. For completeness, we introduce the enthalpy

$$h = e + p/\rho \tag{35}$$
$$h = c_p T \tag{36}$$

and specific heat at constant pressure, c_p. The specific total energy is defined as

$$e_t = e + \frac{u^2}{2} \tag{37}$$

Equations (29)-(31) are a hyperbolic system of equations, which for the purpose of analyzing them as a system, we will write as

$$\partial_t \mathbf{q} + \partial_x \mathbf{F} = \mathbf{S} \tag{38}$$

where

$$\mathbf{q} = \begin{pmatrix} \rho a \\ \rho u a \\ \rho e_t a \end{pmatrix} \tag{39}$$

$$\mathbf{F} = \begin{pmatrix} \rho u a \\ (\rho u^2 + p) a \\ u(\rho e_t + p) a \end{pmatrix} \tag{40}$$

and

$$\mathbf{S} = \begin{pmatrix} \dot{m}\ell(x) \\ p\partial_x a \\ -p\partial_t a + \dot{m}\ell(x) e_p \end{pmatrix} \tag{41}$$

To prove that (38) is in fact a hyperbolic system, we begin by writing it in quasilinear form:

$$\partial_t \mathbf{q} + \mathbf{A}\partial_x \mathbf{q} = \mathbf{S} \tag{42}$$

where we have introduced the flux Jacobian

$$\mathbf{A} = \frac{\partial \mathbf{F}}{\partial \mathbf{q}} = \begin{pmatrix} 0 & 1 & 0 \\ \frac{\gamma-3}{2}u^2 & -(\gamma-3)u & \gamma-1 \\ -\gamma u e_t + (\gamma-1)u^3 & \gamma e_t - \frac{3(\gamma-1)u^2}{2} & \gamma u \end{pmatrix} \tag{43}$$

and γ is the ratio of specific heats for the gas. After some algebra, it may be shown that the eigenvalues of (43) are

$$\lambda_1 = u \tag{44}$$

$$\lambda_2 = u + c \tag{45}$$

$$\lambda_3 = u - c \tag{46}$$

where we have introduced the speed of sound, $c = \sqrt{\gamma(\gamma-1)e}$. Clearly the eigenvalues λ_1-λ_3 are always real, therefore (38) is indeed a hyperbolic system.

4.2 Characteristics variable form

Because the eigenvalues are real and distinct, there is a full set of linearly independent eigenvectors, and we can diagonalize the matrix $\mathbf{A}$. After some algebra, it can be shown that right eigenvectors may be given as the columns of the modal matrix

$$\mathbf{M} = \sqrt{\frac{\rho}{\gamma c_v}} \begin{pmatrix} 1 & \frac{1}{\sqrt{2(\gamma-1)}} & \frac{1}{\sqrt{2(\gamma-1)}} \\ u & \frac{u+c}{\sqrt{2(\gamma-1)}} & \frac{u-c}{\sqrt{2(\gamma-1)}} \\ u^2/2 & \frac{u^2/2+c^2/(\gamma-1)+cu}{\sqrt{2(\gamma-1)}} & \frac{u^2/2+c^2/(\gamma-1)-cu}{\sqrt{2(\gamma-1)}} \end{pmatrix} \tag{47}$$

The rows of $\mathbf{M}^{-1}$ contain the left eigenvectors, namely

$$\mathbf{M}^{-1} = \begin{pmatrix} \sqrt{\frac{\gamma c_v}{\rho}}\left(1 - \frac{(\gamma-1)u^2}{2c^2}\right) & \sqrt{\frac{\gamma c_v}{\rho}}(\gamma-1)u/c^2 & -\sqrt{\frac{\gamma c_v}{\rho}}(\gamma-1)/c^2 \\ -\alpha u\left(1 - \frac{(\gamma-1)u}{2c}\right)/(2c) & \alpha\left(1 - \frac{(\gamma-1)u}{c}\right)/(2c) & \alpha(\gamma-1)/(2c^2) \\ \alpha u\left(1 + \frac{(\gamma-1)u}{2c}\right)/(2c) & -\alpha\left(1 + \frac{(\gamma-1)u}{c}\right)/(2c) & \alpha(\gamma-1)/(2c^2) \end{pmatrix} \tag{48}$$

where

$$\alpha = \sqrt{\frac{2\gamma(\gamma-1)c_v}{\rho}}$$

If we premultiply (42) by $\mathbf{M}^{-1}$, we obtain

$$\mathbf{M}^{-1}\partial_t \mathbf{q} + \mathbf{M}^{-1}\mathbf{A}\mathbf{M}\mathbf{M}^{-1}\partial_x \mathbf{q} = \mathbf{M}^{-1}\mathbf{S} \tag{49}$$

Note that (47) and (48) diagonalize the flux Jacobian: we can write

$$\mathbf{\Lambda} = \mathbf{M}^{-1}\mathbf{A}\mathbf{M} = \begin{pmatrix} \lambda_1 & 0 & 0 \\ 0 & \lambda_2 & 0 \\ 0 & 0 & \lambda_3 \end{pmatrix} \tag{50}$$

If we define

$$\delta\hat{\mathbf{q}} = \mathbf{M}^{-1}\delta\mathbf{q} \equiv \frac{\partial\hat{\mathbf{q}}}{\partial\mathbf{q}}\delta\mathbf{q}$$

then we can write the quasi-one-dimensional equations in decoupled form as

$$\partial_t\hat{\mathbf{q}} + \mathbf{\Lambda}\partial_x\hat{\mathbf{q}} = \hat{\mathbf{S}} \tag{51}$$

where $\hat{\mathbf{S}} \equiv \mathbf{M}^{-1}\mathbf{S}$. The variables $\hat{\mathbf{q}}$ are known as the characteristics variables and they are associated with the propagation of waves. Assuming that u is positive when running downstream (in the direction of increasing x), for a subsonic flow, $u < c$ and we have one wave running upstream with a speed of λ_3, and two waves running downstream with speeds of λ_1 and λ_2. For supersonic flows, all three eigenvalues are positive, therefore all three waves run downstream. When discretizing a hyperbolic system, it is crucial to incorporate these wave speeds in the discretization and the boundary conditions.

In order to concentrate on the strategy we use to couple the combustion chamber model with the nozzle model, we defer discussing the discretization until Section 4.6. There are other forms of the governing equations that are useful, which are obtained by a change of dependent variable. We review these forms next.

4.3 Primitive variable form

We define a set of nonconservative primitive variables

$$\mathbf{v} = \begin{pmatrix} \rho a \\ u a \\ p a \end{pmatrix} \tag{52}$$

After applying the chain rule, to (42), we obtain

$$\frac{\partial \mathbf{q}}{\partial \mathbf{v}} \partial_t \mathbf{v} + \mathbf{A} \frac{\partial \mathbf{q}}{\partial \mathbf{v}} \partial_x \mathbf{v} = \mathbf{S}$$

or, after multiplication by the inverse of the transformation matrix,

$$\partial_t \mathbf{v} + \check{\mathbf{A}} \partial_x \mathbf{v} = \check{\mathbf{S}} \tag{53}$$

where

$$\check{\mathbf{A}} = \frac{\partial \mathbf{v}}{\partial \mathbf{q}} \mathbf{A} \frac{\partial \mathbf{q}}{\partial \mathbf{v}} \tag{54}$$

$$\check{\mathbf{S}} = \frac{\partial \mathbf{v}}{\partial \mathbf{q}} \mathbf{S} \tag{55}$$

Direct differentiation of (52) yields

$$\frac{\partial \mathbf{q}}{\partial \mathbf{v}} = \begin{pmatrix} 1 & 0 & 0 \\ u & \rho & 0 \\ \frac{1}{2}u^2 & \rho u & 1/(\gamma - 1) \end{pmatrix} \tag{56}$$

The inverse of this matrix may be written as

$$\frac{\partial \mathbf{v}}{\partial \mathbf{q}} = \begin{pmatrix} 1 & 0 & 0 \\ -u/\rho & 1/\rho & 0 \\ \frac{1}{2}(\gamma - 1)u^2 & -(\gamma - 1)u & \gamma - 1 \end{pmatrix} \tag{57}$$

It can be verified by direct matrix multiplication that

$$\check{\mathbf{A}} = \begin{pmatrix} u & \rho & 0 \\ 0 & u & 1/\rho \\ 0 & \gamma p & u \end{pmatrix} \tag{58}$$

$$\check{\mathbf{S}} = \begin{pmatrix} 0 \\ e(\gamma - 1)\partial_x a \\ -up(\gamma - 1)\partial_x a \end{pmatrix} \tag{59}$$

4.4 Entropy variable form

When a hyperbolic system is written in entropy variable form, it has special properties that make it amenable to analysis. For example, the flux Jacobians become symmetric. To begin, the entropy is defined as the convex function

$$H = H(\mathbf{q}) = -\rho s \tag{60}$$

where

$$s = \frac{R}{\gamma - 1} \ln\left(\frac{T}{T_r}\right) - R \ln\left(\frac{\rho}{\rho_r}\right) \tag{61}$$

where T_r and ρ_r are the reference values for temperature and density. The entropy variables are defined as

$$\mathbf{w} = (\frac{\partial H}{\partial \mathbf{q}})^t = \frac{1}{T}\begin{pmatrix} -e_t + e(\gamma + 1 - s) \\ u \\ -1 \end{pmatrix} \tag{62}$$

With the variables $\mathbf{w}$ defined, we can write $\mathbf{q}$ in terms of $\mathbf{w}$ as

$$\mathbf{q} = \rho T \begin{pmatrix} -w_3 \\ w_2 \\ 1 - w_2^2/(2w_3) \end{pmatrix} \tag{63}$$

Next, we compute the Jacobian

$$\tilde{\mathbf{A}}_0 \equiv \frac{\partial \mathbf{q}}{\partial \mathbf{w}} = \frac{\rho}{c_v(\gamma - 1)} \begin{pmatrix} 1 & u & e_t \\ u & (\gamma - 1)e + u^2 & u(u^2/2 + \gamma e) \\ e_t & u(u^2/2 + \gamma e) & u^4/4 + \gamma u^e + \gamma e^2 \end{pmatrix} \tag{64}$$

Note that $\tilde{\mathbf{A}}_0$ is symmetric, and positive definite[3]. We now perform a change of dependent variables from $\mathbf{q}$ to $\mathbf{w}$ on (42) and obtain

$$\tilde{\mathbf{A}}_0 \partial_t \mathbf{w} + \tilde{\mathbf{A}} \partial_x \mathbf{w} = \mathbf{S} \tag{65}$$

where $\tilde{\mathbf{A}} = \mathbf{A}\tilde{\mathbf{A}}_0$ is symmetric. The development that follows does not depend upon the precise functional form of $\tilde{\mathbf{A}}$, therefore we do not present it here. The interested reader is referred to Shakib[3]. We do need the matrix $\tilde{\mathbf{A}}_0^{-1} = \frac{\partial \mathbf{w}}{\partial \mathbf{q}}$, however and so we write it here as

$$\tilde{\mathbf{A}}_0^{-1} = \frac{c_v}{\rho e^2} \begin{pmatrix} u^4/4 + \gamma e^2 & -u^3/2 & u^2/2 - e \\ -u^3/2 & u^2 + e & -u \\ u^2/2 - e & -u & 1 \end{pmatrix} \tag{66}$$

4.5 Boundary conditions

4.5.1 Inlet

At an inlet to Ω_f, we enforce a subsonic inflow boundary condition. There are two incoming waves associated with λ_1 and λ_2, therefore we specify two boundary conditions. We choose to specify the total pressure

$$p_t = p\left(1 + \frac{\gamma - 1}{2} M^2\right)^{\frac{\gamma}{\gamma - 1}} \tag{67}$$

and total energy, e_t. In (67), we have introduced the Mach number,

$$M = \frac{|u|}{c}$$

Note that specifying p_t and e_t leaves the velocity (and therefore the mass flux) to be obtained as part of the solution.

4.5.2 Exit

At a given point in time, the exit flow may be subsonic or supersonic. In the supersonic case, there is no boundary condition to enforce, because all waves are leaving the domain. In the subsonic case, there is one incoming wave associated with λ_3, therefore we specify one boundary condition. We choose to specify the pressure.

4.6 Time discretization

We will initially use a forward Euler explicit time discretization strategy to solve all time-dependent equations because an explicit time integrator is easy to implement on GPUs, and it might be that, because of the GPU implementation, the larger number of timesteps will be offset by the high flop rates obtained by running on the device. Thus, we have

$$\Delta(\bar{\rho}V) = -\Delta t \left(\rho_d u_d a_d\right)^n - \Delta t \left[\int_{\Gamma_p} \dot{m}\, dS\right]^n \tag{68}$$

$$\Delta(\bar{\rho}\bar{e}_t V) = -\Delta t \left(\gamma \rho_d u_d \bar{e}_t a_d\right)^n - \Delta t \left[\int_{\Gamma_p} \dot{m} h_t\, dS\right]^n \tag{69}$$

where, e.g.,

$$\Delta(\bar{\rho}V) = (\bar{\rho}V)^{n+1} - (\bar{\rho}V)^n$$

and the superscript $()^n$ indicates that the expression is to be evaluated at time level n. As described in Section 2, the solution at $n = 0$ is known. For brevity of notation, we will omit the superscript $()^n$ unless it is necessary to specify the time level of evaluation for clarity.

Similarly, we semidiscretize (38) in time and apply the method of weighted residuals over the nozzle volume to obtain

$$\int_{x_0}^{x_e} \phi^t \Delta\mathbf{q}\, dx = \Delta t \left[-\int_{x_0}^{x_e} \phi^t \partial_x \mathbf{F}\, dx + \int_{x_0}^{x_e} \phi^t \mathbf{S}\, dx\right] \tag{70}$$

where x_0 is the location where Γ_p intersects the x axis and x_e is the location of Γ_e, and ϕ is an admissible weighting function. After integrating the flux term on the right hand side of (70) by parts, we obtain

$$\int_{x_0}^{x_e} \phi^t \Delta\mathbf{q}\, dx = \Delta t \left[-\phi^t \mathbf{F}|_{x_e} + \phi^t \mathbf{F}|_{x_0} + \int_{x_0}^{x_e} \partial_x \phi^t \mathbf{F}\, dx + \int_{x_0}^{x_e} \phi^t \mathbf{S}\, dx\right] \tag{71}$$

4.7 Space discretization

Next, we discretize (71) in space using the method of finite elements, and construct the weight ϕ using a basis ψ that is local to each element Ω_e. For Galerkin's method, and an element having N nodes, we approximate $\mathbf{q}$ as

$$\mathbf{q} \simeq \sum_{j=1}^{N} \psi_j^t \mathbf{q}_j \text{ on } \Omega_e$$

where ψ_j is the Lagrange basis function associated with node j and $\mathbf{q}_j$ is the corresponding nodal value. A fully discrete approximation to our quasi-one-dimensional flow equations may now be written as

$$\sum_e \sum_j \int_{\Omega_e} \psi_i^t \psi_j \, dx \Delta \mathbf{q}_j = \Delta t \left[\sum_e \int_{\Omega_e} \partial_x \psi_i^t \mathbf{F} dx + \sum_e \int_{\Omega_e} \psi_i^t \mathbf{S} dx - \psi^t \mathbf{F}|_{x_e} + \psi^t \mathbf{F}|_{x_0} \right] \tag{72}$$

Let

$$\mathbf{\Theta}_{ij}^e = \int_{\Omega_e} \psi_i^t \psi_j \, dx$$

so that

$$\sum_e \sum_j \mathbf{\Theta}_{ij}^e \Delta \mathbf{q}_j = \Delta t \left[\sum_e \int_{\Omega_e} \partial_x \psi_i^t \mathbf{F} \, dx + \sum_e \int_{\Omega_e} \psi_i^t \mathbf{S} \, dx + -\psi^t \mathbf{F}|_{x_e} + \psi^t \mathbf{F}|_{x_0} \right] \tag{73}$$

It is well known that Galerkin's method is inadequate for hyperbolic problems. Accordingly, we introduce a stabilized version of (73),

$$\begin{aligned} \sum_e \sum_j \mathbf{\Theta}_{ij}^e \Delta \mathbf{q}_j = {} & \Delta t \left(-\psi^t \mathbf{F}|_{x_e} + \psi^t \mathbf{F}|_{x_0} \right) + \\ & \Delta t \sum_e \left[\int_{\Omega_e} \partial_x \psi_i^t \mathbf{F} \, dx + \int_{\Omega_e} \psi_i^t \mathbf{S} \, dx - \right. \\ & \left. \int_{\Omega_e} \partial_x \psi^t \mathbf{A} \tau \left(\mathcal{L}_h \mathbf{q} \right) dx - \int_{\Omega_e} \nu \partial_\xi \psi^t D_\xi \mathbf{q} dx \right] \end{aligned} \tag{74}$$

The fourth term on the right hand side of (74) is a residual-based, streamline-upwind stabilization term that depends on τ, which is the matrix of intrinsic time scales. The last term in the equation is a discontinuity-capturing operator (DCO) with a nonlinear viscosity coefficient

$$\nu = \min \left(\hat{\nu}, 2(|u| + c)/\ell \right) \tag{75}$$

$$\hat{\nu} = \left(\frac{\mathcal{L}_h \mathbf{q}^t \mathbf{A}_0^{-1} \mathcal{L}_h \mathbf{q}}{\rho R + D_\xi \mathbf{w}^t \mathbf{A}_0 D_\xi \mathbf{w}} \right)^{\frac{1}{2}} \tag{76}$$

where $D_\xi()$ indicates the discrete derivative with respect to the computational coordinates, i.e.

$$D_\xi() = D_\xi x D_x()$$

Note that the numerator of (76) has units of entropy over time squared, and the denominator has units of entropy, so that $\hat{\nu}$ has units of 1/time.

To define the discrete residual, $\mathcal{L}_h\mathbf{q}$, which appears in (74), we begin with the continuous residual in entropy variable form

$$\mathcal{L}\mathbf{q} = \tilde{\mathcal{L}}\mathbf{w} = \tilde{\mathbf{A}}_0\partial_t\mathbf{w} + \tilde{\mathbf{A}}\partial_x\mathbf{w}(\mathbf{q}) - \mathbf{S} = 0 \tag{77}$$

But we also have that

$$\partial_t\mathbf{q} + \partial_x\mathbf{F}(\mathbf{q}) - \mathbf{S} = 0 \tag{78}$$

or

$$\mathbf{S} = \partial_t\mathbf{q} + \partial_x\mathbf{F}(\mathbf{q}) \tag{79}$$

Upon substitution of (79) into (77), we see that

$$\mathcal{L}\mathbf{q} = \tilde{\mathbf{A}}_0\partial_t\mathbf{w} + \tilde{\mathbf{A}}\partial_x\mathbf{w}(\mathbf{q}) - \partial_t\mathbf{q} - \partial_x\mathbf{F}(\mathbf{q}) = 0 \tag{80}$$

since

$$\tilde{\mathbf{A}}_0\partial_t\mathbf{w} = \partial_t\mathbf{q}$$

we may write

$$\mathcal{L}\mathbf{q} = \tilde{\mathbf{A}}\partial_x\mathbf{w}(\mathbf{q}) - \partial_x\mathbf{F}(\mathbf{q}) = 0 \tag{81}$$

We may therefore compute the discrete residual as

$$\mathcal{L}_h\mathbf{q} = \tilde{\mathbf{A}}D_x\mathbf{w}(\mathbf{q}) - D_x\mathbf{F}(\mathbf{q}) = 0 \tag{82}$$

The advantage of writing the residual in this way is that it avoids both the evaluation of the time derivative and the source term.

Finally, the matrix of intrinsic time scales is given by

$$\begin{aligned} \tau &= \left|D_x\xi\mathbf{A}\right|^{-1} && (83)\\ &= \mathbf{M}\left|D_x\xi\mathbf{\Lambda}^{-1}\right|\mathbf{M}^{-1} && (84) \end{aligned}$$

We remark that for the one-dimensional linear Lagrange basis, if we choose a master element such that $\xi \in [-1, 1]$, and the element mapping is isoparametric, then $|D_x\xi| = 2/\ell$, where ℓ is the length of the element in physical coordinates, x. Hence, we may write

$$\tau = \frac{\ell}{2}\mathbf{M}\begin{pmatrix} \frac{1}{|u|} & 0 & 0 \\ 0 & \frac{1}{|u+c|} & 0 \\ 0 & 0 & \frac{1}{|u-c|} \end{pmatrix}\mathbf{M}^{-1} \tag{85}$$

To avoid issues associated with division by zero at sonic and stagnation points, we recognize that the product $\mathbf{A}\tau$ is needed, where

$$\mathbf{A}\tau = \frac{\ell}{2}\mathbf{M}\mathbf{\Lambda}\mathbf{M}^{-1}\mathbf{M}|\mathbf{\Lambda}|^{-1}\mathbf{M}^{-1} = \frac{\ell}{2}\mathbf{M}\,\mathrm{sgn}\,(\mathbf{\Lambda})\,\mathbf{M}^{-1} \tag{86}$$

where $\mathrm{sgn}(x)$ is the signum of x and

$$\mathrm{sgn}\,(\mathbf{\Lambda}) = \begin{pmatrix} \mathrm{sgn}(u) & 0 & 0 \\ 0 & \mathrm{sgn}(u+c) & 0 \\ 0 & 0 & \mathrm{sgn}(u-c) \end{pmatrix}$$

Summarizing, the finite element formulation is given by (74) , with the DCO given by (75) and $\mathbf{A}\tau$ given by (86). The calculation of $\hat{\nu}$ as shown in (76) involves the spatial gradient of the primitive variables, $\mathbf{v}$, in the numerator, and the spatial gradient of the entropy variables, $\mathbf{w}$, in the denominator.

4.8 Discrete boundary conditions

It is possible to examine the signs of λ_i at a boundary and apply the appropriate boundary condition type. We do this at the nozzle exit because we want the flow to be able to evolve from subsonic to supersonic. At $x = x_0$ we enforce a subsonic inflow condition.

We apply boundary conditions on (74) weakly. This means that we must evaluate the fluxes $\mathbf{F}|_{x_e}$ and $\mathbf{F}|_{x_0}$ at a state that is consistent with the prescribed boundary data and the outgoing waves. We find this state by solving a local nonlinear problem. This process is perhaps best illustrated by example.

4.8.1 Subsonic inflow

Recall from Section 4.5.1 that there are two incoming waves and we choose to specify the total pressure and total energy. The outgoing wave is associated with λ_3. We specify $p_t = \bar{p}_t$ and $e_t = \bar{e}_t$. Accordingly, we form the system of equations

$$\begin{pmatrix} p_t - \bar{p}_t \\ e_t - \bar{e}_t \\ \delta\hat{q}_3 \end{pmatrix} = \mathbf{0} \tag{87}$$

and perform a Newton iteration over the index k using

$$\begin{pmatrix} \frac{\partial p_t}{\partial \mathbf{q}} \\ \frac{\partial e_t}{\partial \mathbf{q}} \\ \mathbf{l}_3 \end{pmatrix}^k \delta\mathbf{q}^k = - \begin{pmatrix} p_t^k - \bar{p}_t \\ e_t^k - \bar{e}_t \\ \delta\hat{q}_3^k \end{pmatrix} \tag{88}$$

where $\mathbf{l}_3$ is the third left eigenvector given by the third row of (48), and we have used the fact that $\delta\hat{q}_3 = \mathbf{l}_3\delta\mathbf{q}$. We compute $\delta\hat{q}_3^k$ according to

$$\delta\hat{q}_3^k = \mathbf{l_3^k}(\mathbf{q^k} - \mathbf{q^0}) \tag{89}$$

The row vector $\frac{\partial p_t}{\partial \mathbf{q}}$ is a very complicated expression because (67) has a complex dependence on $\mathbf{q}$. Since the flow is subsonic, for the purposes of the iteration strategy, we compute the derivative $\frac{\partial p_t}{\partial \mathbf{q}}$ using the incompressible approximation

$$p_t = p + \rho u^2/2$$

We emphasize that this approximation is only done for the left hand side of (88). This leads to the row vector

$$\frac{\partial p_t}{\partial \mathbf{q}} = \big((\gamma-2)u^2/2, (2-\gamma)u, \gamma - 1\big) \tag{90}$$

We also have

$$\frac{\partial e_t}{\partial \mathbf{q}} = (-e_t/\rho, 0, 1/\rho) \tag{91}$$

We start the iteration by computing p_t^0 and e_t^0 using the state of the gas as known at the most current solution and update using

$$\mathbf{q}^{k+1} = \mathbf{q}^k + \delta\mathbf{q}^k$$

4.8.2 Subsonic outflow

At a subsonic outflow, there are two outgoing waves and one incoming wave, which is associated with λ_3. In this case, we specify the exit pressure, p_e, and solve

$$\begin{pmatrix} \mathbf{l}_1 \\ \mathbf{l}_2 \\ \frac{\partial p}{\partial \mathbf{q}} \end{pmatrix}^k \delta\mathbf{q}^k = - \begin{pmatrix} \delta\hat{q}_1^k \\ \delta\hat{q}_2^k \\ p^k - p_e \end{pmatrix} \tag{92}$$

with

$$\frac{\partial p}{\partial \mathbf{q}} = \big((\gamma-1)u^2/2, -(\gamma-1)u, \gamma-1\big) \tag{93}$$

In (92), $\delta\hat{q}_1^k$ and $\delta\hat{q}_2^k$ are computed in the manner suggested by (89).

4.8.3 Supersonic outflow

At a supersonic outflow, there are no incoming waves, and so the solution is unconstrained: the fluxes at the boundary are computed using the most recently known state.

References

[1] Tim Kibbey. Trades solid and hybrid motor study statement. Unpublished project notes, 2018.

[2] John D. Anderson Jr. *Modern Compressible Flow, with Historical Perspective*, chapter 5. McGraw-Hill, 1982.

[3] Farzin Shakib. A new finite element formulation of computational fluid dynamics: X. the compressible euler and Navier-Stokes equations. *Computer methods in applied mechanics and engineering*, 89:141–219, 1991.